Parametric optimization of TMD inerter for vibration control of vehicle suspension

Pedro C. Gomes[1], Marcus V. G. de Morais[1]

[1]*Dept. of Mechanical Engineering, Faculty of Technology, University of Brasilia*
Campus Darcy Ribeiro, Asa Norte, 70.910-900, DF, Brazil
enmpedrogomes@gmail.com, mvmorais@unb.br

Abstract. In Tuned Mass Damper (TMDs), the increase of mass increases the effectiveness and frequency band of vibration control. To get around this difficulty, Smith [1] [2] propose a new device called inerter to automobile suspension. The present work aims to determine the optimal parameters for a Tuned Mass Damper Inerter (TMDI) applied in a discrete model of quarter-car suspension for comfort and roadhold criteria. The addition of a parallel TMDI configuration result in a better performance only to low frequencies (0-5Hz).

Keywords: TMD, Inerter, Optimization, Quarter-car suspension.

1 Introduction

TMD concept is a popular passive vibration control strategy for dynamically excited civil structures and mechanical systems Frahm [3]. The theme is extensively applied in engineering problems, as reported in literature review works for applications in civil structural engineering Elias and Matsagar [4], wind turbine Zuo, Bi, and Hao [5] Di Paolo, Nuzzo, Caterino, and Georgakis [6] and non-linear dynamics Lu, Wang, Zhou, and Lu [7] Palomares, Nieto, Morales, Chicharro, and Pintado [8].

Smith [1] [2] proposed a new mechanical device called inerter. Inspired by the constraints of the mechanical correspondent for the capacitor in the mechanical-electrical analogy Firestone [9], Smith Smith [1] defines the inerter concept for the force-current analogy, and establishes the potential for controlling vibration. It is a mechanical device with two terminals that generate equal forces in opposite directions that are proportional to the relative acceleration between the terminals, i.e., $F_i = b(\dot{v}_2 - \dot{v}_1)$, where $b\ [kg]$ is the inertance. The first inerter prototypes used racks associated with gears and/or flywheel Smith [1] Madhamshetty and Manimala [10] Petrini, Giaralis, and Wang [11], other configurations were presented by Smith [2]. The use of gear ratios and flywheel geometrics increase inertance without increasing the mass ratio of the TMD. This feature is of great value to the automobile industry given the consumption and performance restrictions.

The present work aims to determinate the optimal parameters for an inerter type dynamic vibration absorber used in vehicular suspension. Using a model of quarter-car suspension, a sort of parametric optimization by brute force was applied to do a response map of comfort and roadhold criteria. The inerter performance was assessed by report to reduced efficiency limit of ISO 8608 [12]. The addition of a parallel TMDI results in a better performance only to low frequencies (0-5Hz).

2 Quarter-Car Model with an Inerter in Parallel

This chapter presents the equation of the dynamic linear model of quarter-car with an inerter in parallel, and the transferability and roadhold functions Gillespie [13] using the impedance matrix technique. To proceed with the response map optimization technique (section 3), the fundamental equations are dimensionless to reduce the number of optimization parameters. The quarter-car model was used with the parallel inerter, as shown in Figure 1 is due to its easy adaptation to a real vehicle.

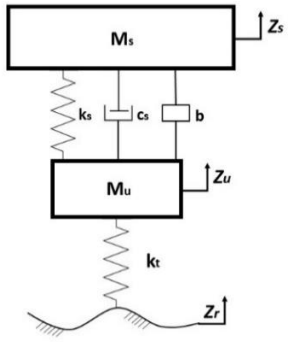

Figure 1 – Quarter-car model with parallel inerter.

By analyzing the dynamic model, described in Figure 1, the movement equations in matrix form can be written as follows

$$\begin{bmatrix} b+M_s & -b \\ -b & b+M_u \end{bmatrix}\begin{Bmatrix} \ddot{z}_s \\ \ddot{z}_u \end{Bmatrix} + \begin{bmatrix} c_s & -c_s \\ -c_s & c_s \end{bmatrix}\begin{Bmatrix} \dot{z}_s \\ \dot{z}_u \end{Bmatrix} + \begin{bmatrix} k_s & -k_s \\ -k_s & k_s+k_t \end{bmatrix}\begin{Bmatrix} z_s \\ z_u \end{Bmatrix} = \begin{Bmatrix} 0 \\ z_r k_t \end{Bmatrix} \qquad (1)$$

where, $\boldsymbol{z}$ is the displacement vector, $\dot{\boldsymbol{z}}$ is the velocity vector and, $\ddot{\boldsymbol{z}}$ is the acceleration vector, and $\boldsymbol{f}(t)$ is the forcing vector. The mass, damping, and stiffness matrices are named, respectively, $\boldsymbol{M}$, $\boldsymbol{C}$ e $\boldsymbol{K}$.

Assuming an excitation $\boldsymbol{f}(t) = \boldsymbol{f}(\omega)\, e^{i\omega t}$, the solution for the steady state is described by $\boldsymbol{K}_d\boldsymbol{z}(\omega) = \boldsymbol{f}(\omega)$, the dynamic rigidity being $\boldsymbol{K}_d = \boldsymbol{K} + i\omega\boldsymbol{C} - \omega^2\boldsymbol{M}$, the displacement vector being $\boldsymbol{z}(t) = \lceil z_s(t) \quad z_u(t)\rceil^T = \boldsymbol{z}(\omega)e^{i\omega t}$ is function of the steady state displacement vector $\boldsymbol{z}(\omega) = {\boldsymbol{K}_d}^{-1} F(\omega)$ and the dynamic force, $\boldsymbol{f}(t) = \lceil 0 \quad z_u k_t\rceil^T = \boldsymbol{f}(\omega)e^{i\omega t}$ is a function of the steady state of the force $\boldsymbol{f}(\omega) = \lceil 0 \quad \mathrm{Z_r}(\omega)\mathrm{k_t}\rceil^T e^{i\omega t}$, corresponding to an excitation with 1 degree of freedom.

The frequency response for the displacement of the sprung mass, also called transmissibility, H_{ST} is described by equation (2). However, for the analysis of comfort in vehicles, displacement is not as crucial factor as acceleration. Therefore, to obtain the frequency response for acceleration, the denominator and numerator must be multiplied by the excitation frequency. Hence, it is concluded that the frequency responses for displacement and acceleration are the same, as described in the following equation.

$$\frac{\ddot{Z}}{\ddot{Z}_r} = H_{ST}(\omega) = \frac{K_1K_2 \; + \; j[K_1C\omega] - \; K_1\beta\omega^2}{det(\boldsymbol{K}_d)} \qquad (2)$$

where: mass ration $\chi = m_u/m_s$; natural frequencies of the unsprung mass $K_1 = \omega_u^2\, \chi = k_u/m_s$ ($\omega_u^2 = k_u/m_u$); natural frequencies of the sprung mass $K_2 = k_s/m_s$ ($\omega_s^2 = k_s/m_s$); damping ratio $C = c_s/m_s$ ($2\xi_s\omega_s = c_s/m_s$); is the inertance ration $\beta = b/m_s$; and the determinant of the impedance matrix $\det(\boldsymbol{K}_d) = [(\beta + \beta\chi + \chi)\omega^4 - (K_2 + \beta K_2 + K_1 + K_1\chi)\omega^2 + K_1K_2] \; + j[\, K_1C\omega - \omega^3C\,(1+\chi)]$.

And the roadhold frequency response corresponds to the analysis of the variation of normal force in tires as a function of frequency, which is calculated from the relative displacement of the unsprung mass with the road $Z_u - Z_r$, that is:

$$\frac{Z_u - Z_r}{Z_r} = H_{ST}(\omega) \; - \; 1 \qquad (3)$$

The transmissibility (2) and the roadhold (3) were used to analyze the frequency response behavior with and without inerter ($b \; = \; 0$).

The movement equations(1) was made dimensionless to enable the choice of the optimal parameters of the quarter-car model with less variation of parameters. Hence, the following dimensionless equation of motion was made (4), where the inertance ratio $\beta = b/m_s$, a mass ratio $\chi = m_u/m_s$, and stiffness ratio $\gamma = k_u/k_s$:

$$\begin{bmatrix} \beta+1 & -\beta \\ -\beta & \beta+\chi \end{bmatrix}\begin{Bmatrix} \ddot{z}_s \\ \ddot{z}_u \end{Bmatrix} + 2\xi\omega_s\begin{bmatrix} 1 & -1 \\ -1 & 1 \end{bmatrix}\begin{Bmatrix} \dot{z}_s \\ \dot{z}_u \end{Bmatrix} + \omega_s^2\begin{bmatrix} 1 & -1 \\ 1 & (1+\gamma) \end{bmatrix}\begin{Bmatrix} z_s \\ z_u \end{Bmatrix} = \omega_s^2\begin{Bmatrix} 0 \\ z_r\,\gamma \end{Bmatrix} \qquad (4)$$

Assuming an excitation $\boldsymbol{f}(t) = \omega_s^2[0 \quad z_r\gamma]^T = \boldsymbol{f}(\omega)\, e^{i\omega t} = \omega_s^2[0 \quad \mathrm{Z_r}(\omega)\mathrm{k_t}]^T e^{i\omega t}$ and a particular harmonic solution $\boldsymbol{z}(t) = [z_s(t) \quad z_u(t)]^T = \boldsymbol{z}(\omega)e^{i\omega t} = [Z_s(\omega) \quad Z_u(\omega)]^T e^{i\omega t}$, the equation of motion in frequency is given by $\boldsymbol{K}_d\boldsymbol{z}(\omega) = \boldsymbol{f}(\omega)$, being the dynamic rigidity $\boldsymbol{K}_d = \boldsymbol{K} + i\omega\boldsymbol{C} - \omega^2\boldsymbol{M}$. Therefore, taking the frequency ratio (r) as the excitation frequency ratio by the natural frequency we have:

$$\left\{r^2\begin{bmatrix}1 & -1\\ 1 & (1+\gamma)\end{bmatrix} + 2\xi r\imath\begin{bmatrix}1 & -1\\ -1 & 1\end{bmatrix} - \begin{bmatrix}\beta+1 & -\beta\\ -\beta & \beta+\chi\end{bmatrix}\right\}\begin{Bmatrix}Z_s\\ Z_u\end{Bmatrix} = r^2\begin{Bmatrix}0\\ z_r\,\gamma\end{Bmatrix} \qquad (5)$$

The dimensionless parameters used are: Υ is the ratio of the stiffness of the tire and the shock absorber; χ is the ratio between the sprung and unsprung masses; β is the ratio of the inertance and the sprung mass; and r is the ratio of the excitation frequency and the natural frequency.

3 Optimization Via Response Map

The parametric optimization scans the dimensionless variables of stiffness ratio (Υ) and mass ratio (χ) for a given frequency ratio (r). Furthermore, for each combination of dimensionless variables, it was searched the best damping ratio (ξ) for the analyzes criterion. This exhaustive process results in a response map for comfort and another for roadhold. Due to the response map, it is possible to carry out a trade-off ("lose-and-win") analysis to seek the most effective combination of vehicle suspension design.

3.1 Random Vibration Notions Applied to the Track PSD

To establish the mathematical rudiments of random vibrations, it was used the works of Alkmim, Fabro, and Morais [14] and Martins, Morais, and Avila [15]. Therefore, the definition of power spectrum density (PSD) $S_{yy}(\omega)$ is done by:

$$S_{yy} = H^*(\omega)H(\omega)S_{xx}(\omega) = |H(\omega)|^2 S_{xx}(\omega) \qquad (6)$$

where, H^* is the conjugate of the transfer function. Due to the Eq. (6) is obtained that the variance for a single input is calculated as:

$$\sigma^2 = \int_0^{+\infty} |H(\omega)|^2 S_{xx}(\omega)\, d\omega \qquad (7)$$

establishing a relationship between the input and output of the PSD. The standard ISO 8608 [12] presents the mathematical model to use road PSD in the simulations, the standard define $G_a(\omega)$ as the acceleration of road PSD that can be substituted in Eq. (7) as $S_{xx}(\omega)$.

3.2 Response Map

Substituting in Eq. (7) the white noise $S_{xx}(\omega) = 1$ and from Eq (2) $H(\omega) = H_{ST}(\omega)$ is obtained:

$$\sigma_s^2 = \int_0^{+\infty} |H_{ST}(\omega)|^2\, d\omega \qquad (8)$$

Therefore, the vibration minimization criterion for the sprung mass $J_1(\chi, \gamma, \xi)$ is given by:

$$J_1(\chi, \gamma, \xi) = min(\sigma_s^2) \qquad (9)$$

Similarly, the response map was constructed aiming the tire contact with the ground (roadhold), however, as an optimization parameter, it was sought the smallest maximum point of the presented transfer function. Since it is desired to obtain the smallest variation of the normal force, in this way, the parameters (χ, γ, ξ) chosen must decrease the maximum amplification of the system, ergo the modulus of Eq. (3) was calculated in order to obtain the transfer function and sought to obtain its maximum value:

$$J_2(\chi, \gamma, \xi) = min\left(max\left|\frac{Z_u - Z_r}{Z_r}\right|\right) \qquad (10)$$

4 Numerical Results

It's presented (i) the optimization of the stiffness, mass and damping parameters of a classic quarter-car model ($b = 0$), and (ii) the parametric optimization of the quarter-car model with inerter in parallel, according to the mathematical model (5). The construction of the response map for comfort J_1 and roadhold J_2 optimization metrics is presented. The response maps produced evaluate the optimal parameters of the vehicle Baja SAE version 2021 of the Piratas do Cerrado team (UnB - FT), whose dimensionless parameters are $\chi = 0.3$, $\gamma = 37$, and $\xi = 0.15$. Furthermore, due to the stiffness ratio parameter γ is modified by the tire pressures, a parametric analysis of the stiffness ratio variation was performed for $\gamma = 30,\ 37,\ 45\ and\ 55$. The analyzes seek to propose modifications to improve the performance of this vehicle.

4.1 Parametric Optimization of the Classic Quarter-Car Model

The comfort response map $J_1(\chi, \gamma, \xi_{opt}) = \min(\sigma_s^2)$ (Figure 2), according to Eq. (9), presents the dynamic response of the sprung mass σ_s^2 of the classic quarter-car model ($b = 0$) for the range of dimensionless parameters of mass ratio $\chi \in [0.05; 0.5]$, stiffness ratio $\gamma \in [5; 100]$ and the damping ratio $\xi \in [0.05; 0.5]$. Figure 3 shows the roadhold response map $J_2(\chi, \gamma, \xi_{opt}) = \min(\max|(Z_u - Z_r)/Z_r|)$, according to Eq. (10),for the same interval of the dimensionless parameters. Since according to Gillespie [13] the allowable damping ratios ξ are $[0.2; 0.40]$ for the cases where the response maps provided damping ratios outside this range, they were replaced by the closest allowable value.

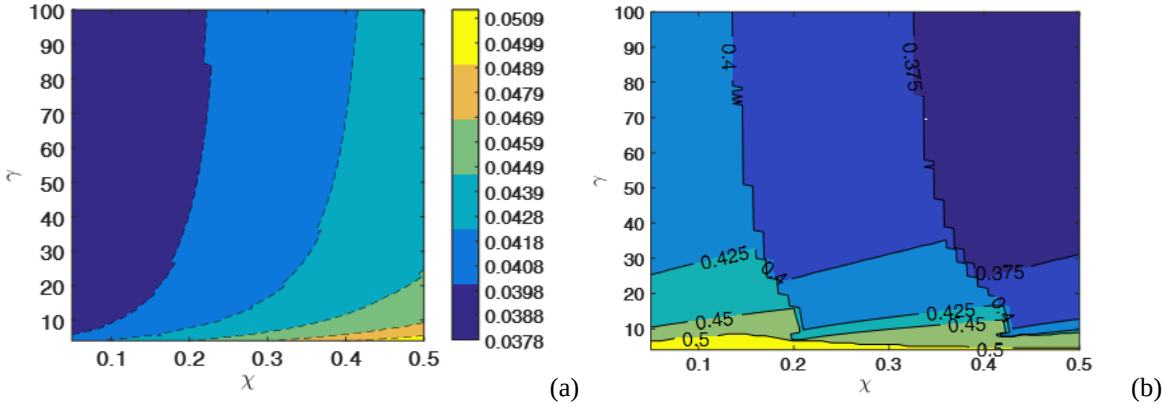

(a) (b)

Figure 2 – Response map of the comfort criterion $J_1(\chi, \gamma, \xi)$: (a) rms acceleration of the sprung mass $\sigma_s^2(\chi, \gamma, \xi_{opt})$, (b) damping ratio ξ_{opt} as a function of the ratios of mass χ and of stiffness γ.

From the response maps, a trade-off conflict was found since the optimization of J_1 for almost all situations implies losses in J_2. Given a mass ratio χ constant, the increase in the stiffness ratio γ causes: (a) a decrease in the rms acceleration value of the sprung mass (improving vehicle comfort), and (b) an increase in the roadhold criterion (worsening driveability).

Figure 4 shows the rms-acceleration of the sprung mass for a 1/3 octave band, the vehicle response was compared with the values of the ISO 2631 [16]. Since it is a competition vehicle, the reduced efficiency limit was chosen to guarantee the pilot's performance. The parameters taken from the response map worsened the maximum exposure time at frequencies above 10Hz, the reason may be the influence of the frequency shift in which the second peak of the transmissibility function occurs.

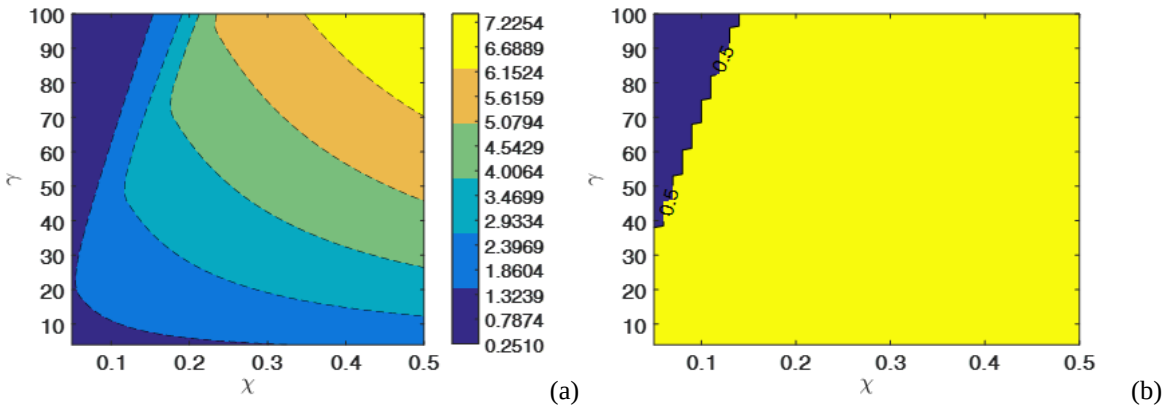

Figure 3 – Response map of the roadhold criterion $J_1(\chi, \gamma, \xi)$: (a) max relative displacement of the unsprung mass $\sigma_s^2(\chi, \gamma, \xi_{opt})$, (b) damping ratio ξ_{opt} as a function of the ratios of mass χ and of stiffness γ

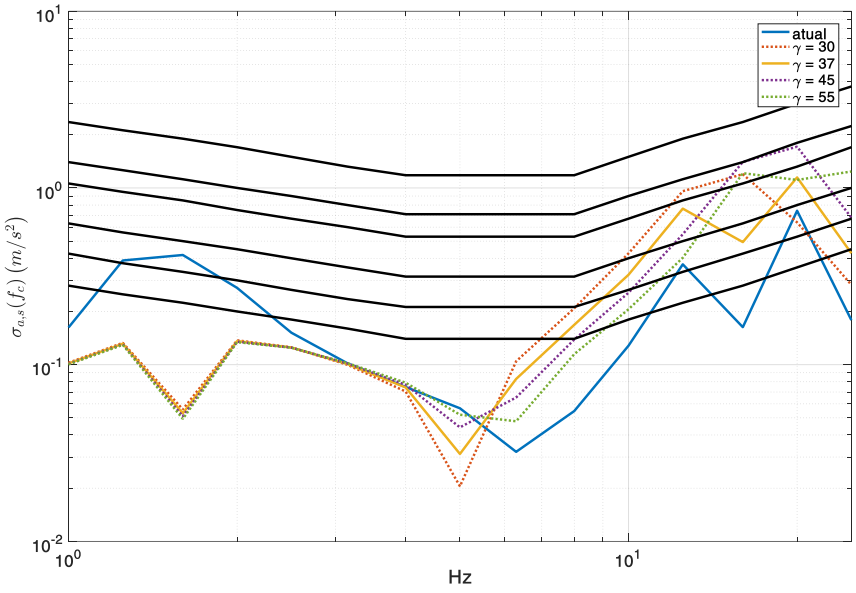

Figure 4 – Analysis of exposure times for the reduced efficiency level according to ISO 2631 [16].

The settings taken from the response map achieved a significant reduce in the roadhold peak, Table 1, which represents a performance improvement. However, from the standard ISO 2631 [16] (Figure 4), the new parameters resulted in a reduction in the maximum number of hours for the pilot to drive without the driver's efficiency level being reduced. Table 1 presents an overview of the analyzed parameters and the results obtained from them.

Table 1 – Comparative of analyzes settings

Setting	J1	J2	Exposition time
atual	0,000382	10,8644	8h
ϒ=30	0,04227	3,173	2h
ϒ=37	0,04247	3,488	4h
ϒ=45	0,04229	3,817	2h
ϒ=55	0,04213	4,191	2h

For the design of the Baja SAE vehicle of Piratas do Cerrado, it is proposed to increase the damping ratio $\xi_{opt} = 0.4$ and maintain the stiffness ratio $\gamma = 37$ and the mass ratio $\chi = 0.30$. Since the maximum value of the roadhold is 3 times lower than the current one and, although the maximum time for the driver to not have reduced efficiency is lower, it is within the desirable 4 hours.

4.2 Quarter-Car Model Parametric Optimization with Inerter

The use of the inerter was evaluated to improve the performance and comfort of the previously optimized vehicle. Hence, the parameters used were damping ratio $\xi_{opt} = 0.4$, stiffness ratio $\gamma = 37$ and mass ratio $\chi = 0.30$. Then, the inertance ratio $\beta \in [0;1]$ was varied, where $\beta = 0$ represents the current configuration of the vehicle suspension without inert.

The performance of the system with inerter was measured from the parameter J_1 and J_2. In addition, from a PSD with the same track as used for the analysis without inerter: (a) rms-acceleration of the sprung mass was calculated for a 1/3 octave band of the suspended mass and from the ISO 2631 [16] standard; (b) the driving hours limit was calculated to avoid a reduced efficiency level

The analyzes showed that the influence of inertance β on both the comfort criterion J_1 and the roadhold criterion J_2 almost does not result in changes when $\beta < 0.1$ and for higher values of inertance there is an exponential worsening in the two criteria of optimization.

Figure 5 evaluates the maximum exposure time to the reduced pilot efficiency limit as a function of the increase in inertance β. It was found that the efficiency limit was maintained at 4h, according to the current configuration. And, with the increase in inertance β, there is a reduction in the efficiency threshold.

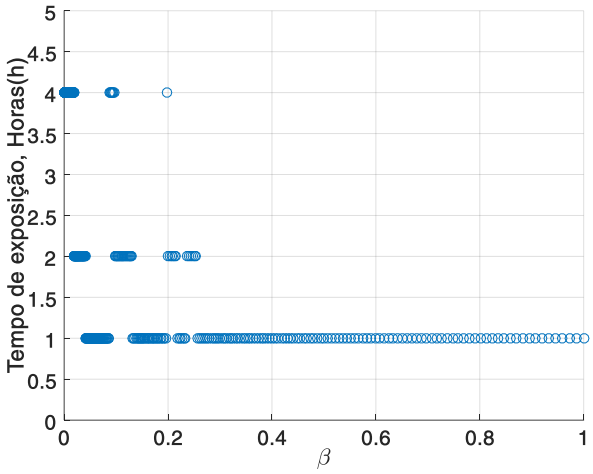

Figure 5 – Analysis of the influence of the inertance ratio (β) on the maximum exposure time for reduced efficiency level according to the standard ISO 2631 [16].

It is concluded that there is no gain when using this configuration with a parallel inerter, in most cases it resulted in a worsening for both J_1 and J_2 criteria. Thereby, it is suggested that the inerter do not be used in this configuration.

5 Conclusions

The present work is done several analyzes to find the optimal parameters of quarter-car suspension model using (or not) an TMDI. The response maps produced evaluate the optimal parameters of the vehicle SAE-Baja version 2021 of Piratas do Cerrado team (UnB - FT) for the dimensionless parameters mass ratio χ = 0.3, stiffness ratio γ = 37, indicated an optimal damping ratio $\xi_{opt} = 0.4$. There was a trade-off problem (optimization with conflicting parameters) that is, the optimization of driveability parameters results in loss of comfort, and vice versa.

As the Baja SAE competition seeks to test the vehicle's limits in an off-road environment, it was decided to optimize the driveability by checking the comfort defined by the ISO 2631 [16].

It was proposed to increase the damping ratio to $\xi_{opt} = 0.4$ and to maintain the stiffness ratio $\gamma = 37$ and the mass ratio $\chi = 0.30$. This way, the roadhold value was reduced, being it 2.5 times smaller than the current one and, although the maximum time for the pilot to not have reduced efficiency is less, it is within the desirable of 4 hours.

Finally, the parametric analysis of the inertance coefficient was performed, which did not result in consistent improvement. The driveability improvements were small for a frequency range restricted to 0 and 5Hz. Furthermore, the loss of comfort was considerable. The parallel inert configuration does not result in improvements in comfort and driveability characteristics, nor in- maximum time without reduced efficiency.

Acknowledgements. This study was funded by the National Council for Research and Development (CNPq) in partnership with the University of Brasília by the Notice 2020/2021 PROIC/UnB-CNPq. The authors thank CNPq and UnB for the resources that made this work possible.

Authorship statement: The authors hereby confirm that they are the sole liable persons responsible for the authorship of this work, and that all material that has been herein included as part of the present paper is either the property (and authorship) of the authors or has the permission of the owners to be included here.

References

[1] M. C. Smith, "Synthesis of mechanical networks: The inerter," *IEEE Trans. Automat. Contr.*, vol. 47, no. 10, pp. 1648–1662, 2002, doi: 10.1109/TAC.2002.803532.
[2] M. C. Smith, "The Inerter Concept and Its Application," *Soc. Instrum. Control Eng. Annu. Conf.*, no. August, p. 40, 2003.
[3] H. Frahm, "Device for damping vibrations of bodies," 1909
[4] S. Elias and V. Matsagar, "Research developments in vibration control of structures using passive tuned mass dampers," *Annu. Rev. Control*, vol. 44, pp. 129–156, Jan. 2017, doi: 10.1016/j.arcontrol.2017.09.015.
[5] H. Zuo, K. Bi, and H. Hao, "A state-of-the-art review on the vibration mitigation of wind turbines," *Renewable and Sustainable Energy Reviews*, vol. 121. Pergamon, p. 109710, Apr. 2020. doi: 10.1016/j.rser.2020.109710.
[6] M. Di Paolo, I. Nuzzo, N. Caterino, and C. T. Georgakis, "A friction-based passive control technique to mitigate wind induced structural demand to wind turbines," *Eng. Struct.*, vol. 232, p. 111744, Apr. 2021, doi: 10.1016/j.engstruct.2020.111744.
[7] Z. Lu, Z. Wang, Y. Zhou, and X. Lu, "Nonlinear dissipative devices in structural vibration control: A review," *J. Sound Vib.*, vol. 423, pp. 18–49, Jun. 2018, doi: 10.1016/j.jsv.2018.02.052.
[8] E. Palomares, A. J. Nieto, A. L. Morales, J. M. Chicharro, and P. Pintado, "Numerical and experimental analysis of a vibration isolator equipped with a negative stiffness system," *J. Sound Vib.*, 2018, doi: 10.1016/j.jsv.2017.11.006.
[9] F. A. Firestone, "A NEW ANALOGY BETWEEN MECHANICAL AND ELECTRICAL SYSTEMS," *J. Acoust. Soc. Am.*, vol. 4, no. 3, pp. 249–267, Jan. 1933, doi: 10.1121/1.1915605.
[10] K. Madhamshetty and J. Manimala, "Low-Rate Characterization of a Mechanical Inerter," *Machines*, vol. 6, no. 3, p. 32, Jul. 2018, doi: 10.3390/machines6030032.
[11] F. Petrini, A. Giaralis, and Z. Wang, "Optimal tuned mass-damper-inerter (TMDI) design in wind-excited tall buildings for occupants' comfort serviceability performance and energy harvesting," *Eng. Struct.*, vol. 204, p. 109904, Feb. 2020, doi: 10.1016/j.engstruct.2019.109904.
[12] ISO 8608, "Mechanical vibration — Road surface profiles — Reporting of measured data," 2016.
[13] T. D. Gillespie, *Fundamentals of Vehicle Dynamics.pdf*, 1st Editio. Sae, 1992.
[14] M. H. Alkmim, A. T. Fabro, and M. V. G. de Morais, "Optimization of a tuned liquid column damper subject to an arbitrary stochastic wind," *J. Brazilian Soc. Mech. Sci. Eng.*, vol. 40, no. 11, pp. 1–11, 2018, doi: 10.1007/s40430-018-1471-3.
[15] J. F. Martins, M. V. G. de Morais, and S. M. Avila, "Experimental study of equivalente 1DoF main structure coupled to TLCD: Validation of optimum parameter obtained by parametric optimization," in *25th ABCM International Congress of Mechanical Engineering*, 2019, no. Unico, pp. 1–4. doi: 10.26678/abcm.cobem2019.cob2019-0812.
[16] ISO 2631, "Guia para avaliação da exposição humana à vibrações de corpo inteiro," 1978.